

Comparative Analysis of Two Well-known Maximum Power Point Tracking Techniques for Photovoltaic Cell

Keerti Yadav
M.Tech. student
Department of EEE
Technocrats Institute of Technology
Bhopal (M. P.) India

Anuprita Mishra
Professor
Department of EEE
Technocrats Institute of Technology
Bhopal (M. P.) India

Abstract—This paper provides a comparative analysis of widely used maximum power point technique (MPPT) i.e. Perturb and observe MPPT and Incremental Conductance MPPT used in photovoltaic application. A boost converter is used to step-up the voltage of the PV cell to a required DC-link voltage. A complete analysis of the boost converter has been described in this paper.

Keywords— PV cell; Boost converter; DC-link; MPPT

I. INTRODUCTION

Due to the limited resources of fossil fuel, the development of renewable energy sources is rising now days. The main advantages of these renewable energy sources are (a) it is plenty of available in nature, (b) eco-friendly and (c) recyclable. There are many renewable energy sources such as wind energy, solar energy, hydro energy and tidal energy. To harness electrical energy from renewable energy sources, power conditioning unit (PCU) is required. PCU comprises of one or more than one power electronic converter (PEC). DC-micro grids (Figure 1) are one of the most useful techniques where the renewable energy source is connected to the load with the help of a DC-bus [1]. Design of DC-micro grid has been studied in [13].

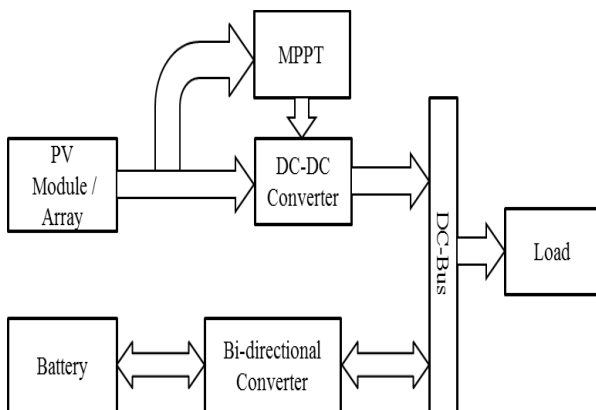


Fig. 1. Block diagram of DC-grid

Photovoltaic cell is one of the most widely used renewable energy. The photovoltaic cell provides electrical energy when solar irradiance is incident on it. To extract maximum power from PV cell, maximum power point tracking technique is used.

This paper provides a detailed design and analysis of two well-known MPPT algorithms such as perturb and observe and

incremental conductance. Both MPPT are hill-climbing algorithm and true MPPT. Simulation results are provided to illustrate the functionality of the MPPT techniques.

This paper is organized as follows. Section II provides the mathematical modeling of PV cell. Section III presents the functionality of different maximum power point tracking algorithms. Section IV presents details of switched mode power converter. Section V provides simulation results. Section VI concludes the paper.

II. MATHEMATICAL MODEL OF PV CELL

The photovoltaic system converts sunlight directly to electricity without having any disastrous effect on our environment. The basic segment of PV array is PV cell, which is just a simple p-n junction device. Figure 2 shows the electrical equivalent circuit of PV cell.

The ideal PV cell consists of a constant current source and a diode whereas the practical PV cell consists of additional series R_s and parallel resistance R_p . Modeling of PV cell is summarized in [2-4].

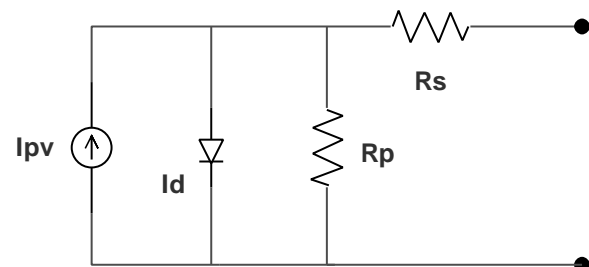


Fig. 2. Circuit diagram of PV cell

The basic equation which describes the I-V characteristics of an ideal PV cell can be represented as

$$I = I_{pv} - I_d \tag{1}$$

Where I_{pv} is current of PV cell and I_d is Shockley diode equation which can be represented as

$$I_d = I_o \left[\exp\left(\frac{qV}{akT}\right) - 1 \right] \tag{2}$$

Therefore, I-V characteristics of an ideal PV cell can be represented as

$$I = I_{pv} - I_o \left[\exp\left(\frac{qV}{akT}\right) - 1 \right] \quad (3)$$

Where I_o the leakage is current of diode, q is electron charge, K is Boltzmann constant and T is temperature of p-n junction (Kelvin)

In practice, the series and parallel equivalent characteristics of PV cell can be represented as

$$I = I_{pv} - I_o \left[\exp\left(\frac{qV}{akT}\right) - 1 \right] - \frac{V + R_s I}{R_p} \quad (4)$$

Where R_s is series resistance and R_p is parallel resistance

V_t is thermal resistance of PV cell and N_s is number of cells connected in series. The thermal resistance of PV cell can be represented as

$$V_t = \frac{N_s k T}{q}$$

The current of the PV cell is dependent on solar irradiance and temperature. The relation between the PV current and temperature can be represented as

$$I_{pv} = (I_{pv,n} + K_I \Delta_T) \frac{G}{G_n} \quad (5)$$

where $I_{pv,n}$ is light generated current at nominal operating condition ($25^\circ\text{C}, 1000\text{W}/\text{m}^2$), Δ_T is the difference of temperature (Actual and nominal temperature), G is the irradiance of the surface and G_n is the nominal irradiance. The relationship of diode saturation current with temperature can be represented as

$$I_o = I_{o,n} \left(\frac{T_n}{T}\right)^3 \exp\left[\frac{qE_g}{ak} \left(\frac{1}{T_n} - \frac{1}{T}\right)\right] \quad (6)$$

The nominal saturation current can be expressed as

$$I_{o,n} = \frac{I_{sc,n}}{\exp\left(\frac{V_{oc,n}}{aV_{t,n}}\right) - 1} \quad (7)$$

The modified nominal saturation current can be represented as

$$I_{o,n} = \frac{I_{sc,n} + K_V \Delta_T}{\exp\left(\frac{V_{oc,n} + K_I \Delta_T}{aV_t}\right) - 1} \quad (8)$$

III. MAXIMUM POWER POINT TRACKING

Maximum Power Point Tracking, frequently referred to as MPPT, is an electronic system that operates the Photovoltaic (PV) modules in a manner that allows the modules to produce all the power they are capable of. MPPT is not a mechanical tracking system that “physically moves” the modules to make them point more directly at the sun. MPPT is a fully electronic system that varies the electrical operating point of the modules so that the modules are able to deliver maximum available

power. Additional power harvested from the modules is then made available as increased battery charge current. MPPT can be used in conjunction with a mechanical tracking system, but the two systems are completely different. Figure 3 displays the concept of MPPT. Figure 4 shows the classification of MPPT algorithms.

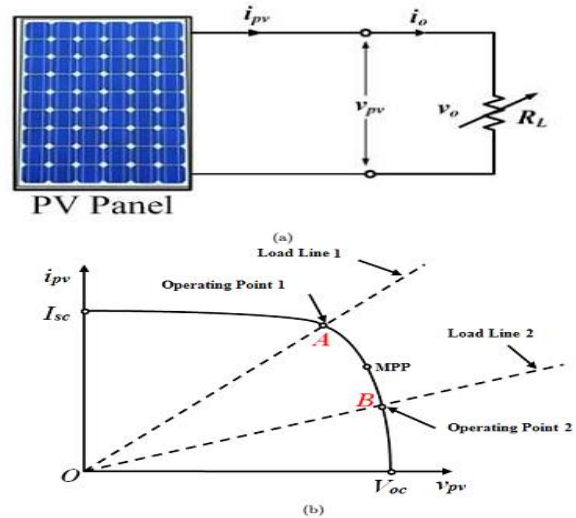


Fig. 3. The concept of MPPT

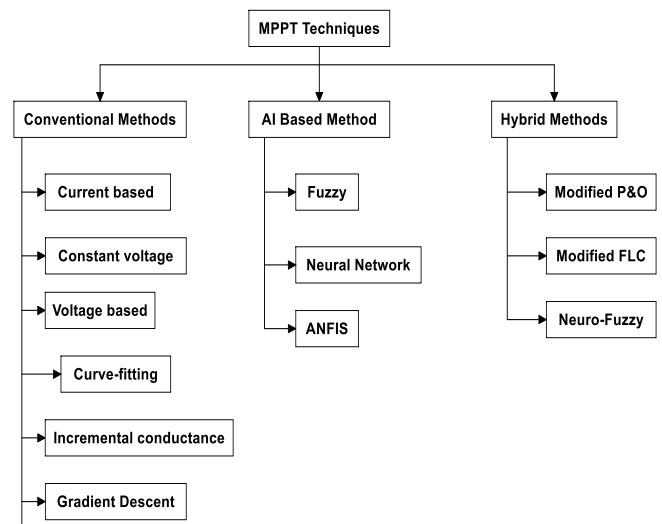


Fig. 4. Classification of different MPPT Techniques

A comparative analysis of different MPPT techniques have been studied in [5-12].

A. Perturb Observe MPPT

One of the most widely used MPPT is Perturb and Observe (P&O) MPPT because it is true MPPT, independent of PV panel, can be implemented using both analog and digital circuit and the technique doesn't require periodic tuning. The

main principle of (P&O) MPPT is the checking of $\frac{dP}{dV}$ slope.

The slope is positive at the left of MPP and the slope is negative at the right of MPP [15]. This can be mathematically expressed as

$$\frac{dP}{dV} = \begin{cases} > 0 & V < V_{mpp} \\ = 0 & V = V_{mpp} \\ < 0 & V > V_{mpp} \end{cases} \quad (9)$$

Initially the voltage and current of PV module is measured using respective voltage and current sensors and the power is calculated. Change of power and change of voltage is calculated and if the change of power $dP > 0$ and also $dV > 0$ then the duty cycle increases by a fraction of ΔD and for negative slope the duty cycle decreases by a fraction of ΔD . Figure 5 shows the flow chart of perturb and observe MPPT.

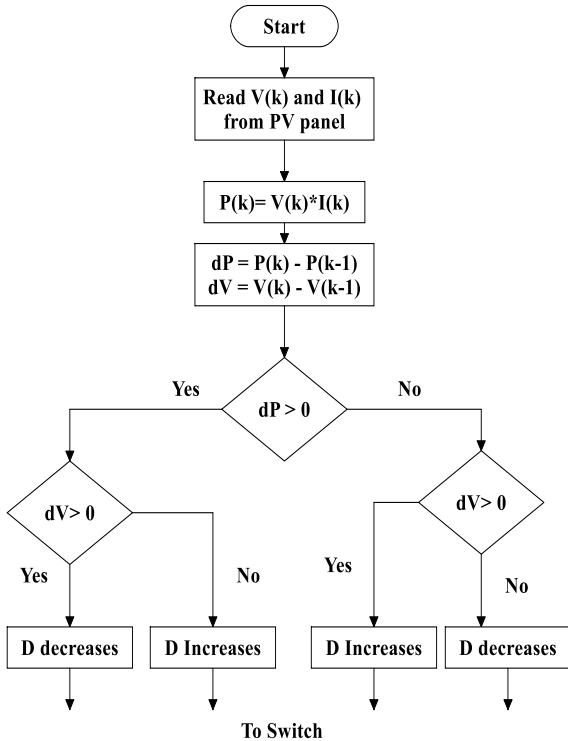


Fig. 5. Flow chart of classical perturb-observe MPPT

B. Incremental Conductance MPPT

Figure 6 shows the flow chart of incremental conductance MPPT. The Incremental conductance method eliminates the drawbacks of the Perturb and Observe method. It uses the advantage that the derivate of the power with respect to the voltage at the maximum power point is zero. The incremental conductance can determine that the MPPT has reached the MPP and stop perturbing the operating point. If this condition is not met, the direction in which the MPPT operating point must be perturbed can be calculated.

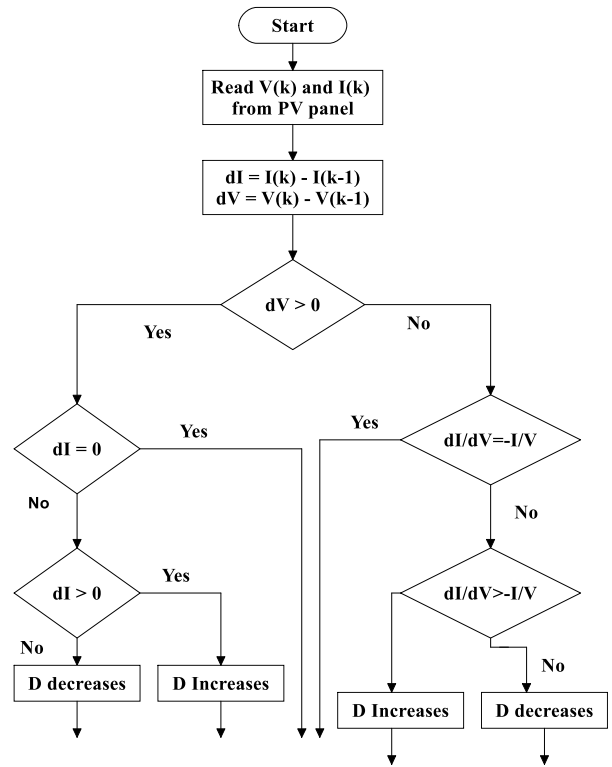


Fig. 6. Flow chart of classical incremental conductance MPPT

The efficiency of MPPT technique can be calculated using the following formula

$$\eta_{mppt} = \frac{P_{pv}}{P_{mppt}} \times 100 \quad (10)$$

IV. POWER ELECTRONIC INTERFACE FOR PV MODULE

Power electronic interface for PV module is illustrated in Figure 7. PEI comprises of sensors, MPPT algorithms, PWM module, DC-DC converter and resistive load.

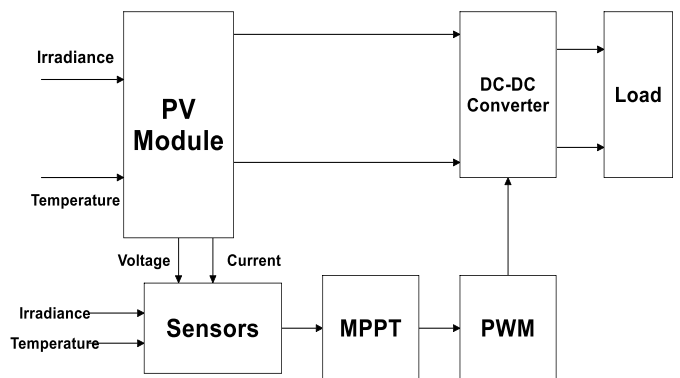


Fig. 7. Block diagram of PEI for PV based generation

The circuit diagram of DC-DC boost converter is shown in Fig. 8. DC-DC boost converter is a non-minimum phase system which means the output voltage to duty cycle transfer function of boost converter has a zero in right half of S-plane. This characteristic makes the controller design more complicated.

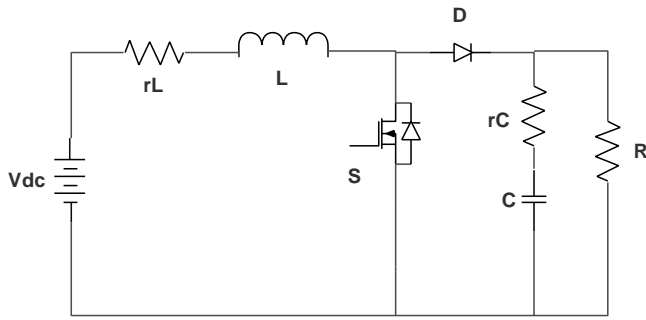


Fig. 8. Circuit diagram of boost converter

The transfer function of boost converter can be represented as

$$G_{boost}(s) = \frac{\tilde{v}_o(s)}{\tilde{d}(s)} = \frac{V_{in}}{(1-D)^2} \left(\frac{(1+s r_c C) \left(1 - s \frac{L}{(1-D)^2 (R-r_i)} \right)}{1 + s \frac{R \{ r_L C (R+r_c) + L \}}{(R+r_c) [r_L + (1-D)^2 R]} + \frac{s^2 L C R}{r_L + (1-D)^2 R}} \right)$$

The resonant frequency of the LC circuit of the converter can

be represented as $\omega_o = \frac{1-D}{\sqrt{LC}}$

The right-half-zero frequency of the converter can be

represented as $\omega_{RHP} = \frac{R^2(1-D)^2}{(R+r_c)L} - \frac{(r_c+r_L)}{L}$

There are different methods to eliminate the RHPZ characteristics. One such method is injected absorbed current method. The transfer function of boost converter using IAC method can be represented as

$$G_{IAC}(s) = \frac{V_{in}}{V_p} \left(\frac{1}{1-D} \right)^2 \left[1 - s \left\{ \left(\frac{1}{1-D} \right)^2 \frac{L}{R} + \frac{DT_s}{2} - T_s \right\} \right] \left[\left(\frac{1}{1-D} \right)^2 \frac{L}{R} + \frac{T_s}{2} \right] + s^2 \left(\frac{LC}{(1-D)^2} \right)$$

V. SIMULATION RESULTS

Figure 9 represents the P-V curve of the PV module under consideration. From the Figure it can deduce that power in PV system is increased at certain point with the voltage. After a certain value of V, the power of the PV system started to fall. This paper considers a SPR-305-WHT PV module. This is manufactured by Sun Power. P-V and V-I characteristics of SPR-305-WHT module with varying solar irradiance is shown in Fig. 10. When 66 parallel strings and 5 series module of the said scheme is connected, the V-I and P-V characteristics of the solar module is shown in Fig. 11. The electrical response of the PV module changes with change in ambient temperature. Fig. 12 shows the P-V and V-I characteristics of the solar module with varying temperature.

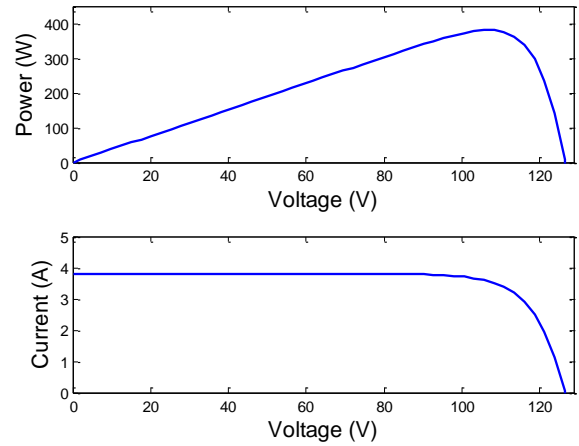


Fig. 9. P-V and V-I plot for PV cell

TABLE I: SPECIFICATION OF SPR-305-WHT PM MODULE

Parameters	Variable	Value
Number of cells per module	N_c	96
Number of series connected module	N_s	4
Number of parallel strings	N_p	1
Open-circuit voltage	V_{oc}	64.2V
Short-circuit current	I_{sc}	5.96 A
Maximum Power	P_{mp}	305W
Series resistance	R_s	0.037998 Ω
Parallel resistance	R_p	993.5 Ω
Saturation current	I_{sat}	1.1753e-8A
Photovoltaic current	I_{ph}	5.9602A

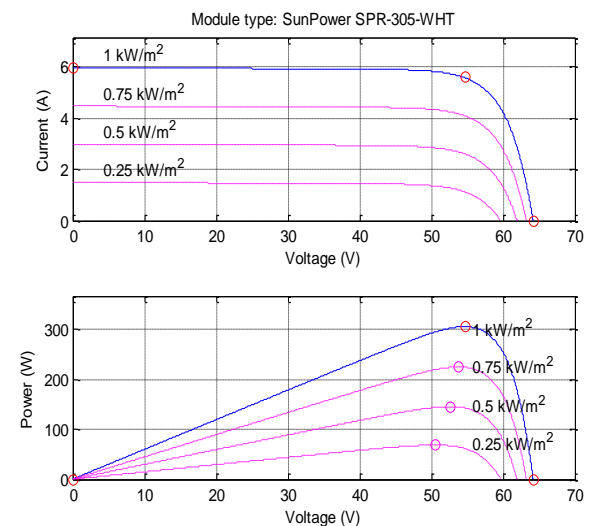


Fig. 10. P-V and V-I characteristics of SPR-305-WHT module

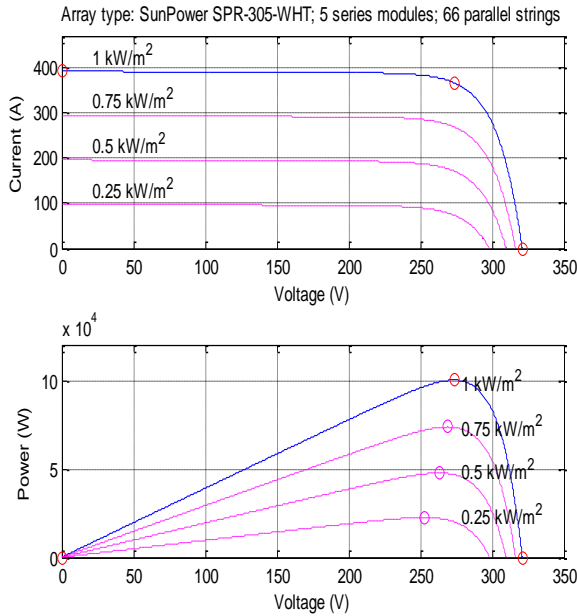


Fig. 11. V-I characteristics of SPR-305-WHT 5 series module and 66 parallel strings

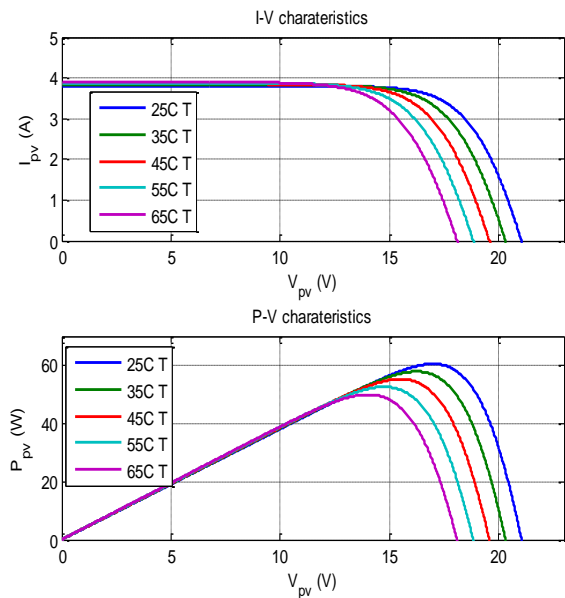


Fig. 12. P-V and V-I plot of PV cell with varying temperature

TABLE II: COMPARISON OF MPPT TECHNIQUES

Parameters	P&O	IC
Control variable	V,I	V,I
Tracking accuracy	Medium	High
Periodic Tuning	No	No
Ability to track true maxima	Yes	Yes
Sensitivity	Medium	Medium
Efficiency	Medium	High

VI. CONCLUSION

This paper provides a detailed analysis and comparative analysis of two well-known MPPT algorithms for PV cell. A 300W PV module is considered and a DC-micro grid has been designed. Detailed simulation results have been provided. The electrical voltage of PV cell gets changed due to change in solar irradiance and ambient temperature. The comparative analysis of two MPPT algorithms are shown using simulation.

REFERENCES

- [1] A. T. Elsayed, A. A. Mohamed, and O. A. Mohammed, "Dc microgrids and distribution systems: An overview," *Electric Power Systems Research*, vol. 119, pp. 407–417, 2015.
- [2] M. G. Villalva, J. R. Gazoli *et al.*, "Comprehensive approach to modeling and simulation of photovoltaic arrays," *IEEE Trans. Power Electron.*, vol. 24, no. 5, pp. 1198–1208, 2009.
- [3] S. A. Rahman, R. Varma, and T. Vanderheide, "Generalised model of a photovoltaic panel," *IET Renewable Power Generation*, vol. 8, no. 3, pp. 217–229, 2014.
- [4] G. Bhuvaneswari and R. Annamalai, "Development of a solar cell model in matlab for pv based generation system," in *Proc. IEEE India Conference (INDICON)*, 2011, pp. 1–5.
- [5] B. Subudhi and R. Pradhan, "A comparative study on maximum power point tracking techniques for photovoltaic power systems," *IEEE Trans. Sustain. Energy*, vol. 4, no. 1, pp. 89–98, 2013.
- [6] P.-C. Chen, P.-Y. Chen, Y.-H. Liu, J.-H. Chen, and Y.-F. Luo, "A comparative study on maximum power point tracking techniques for photovoltaic generation systems operating under fast changing environments," *Solar Energy*, vol. 119, pp. 261–276, 2015.
- [7] M. Berrera, A. Dolara, R. Faranda, and S. Leva, "Experimental test of seven widely-adopted mppt algorithms," in *Proc. IEEE PowerTech*, 2009, pp. 1–8.
- [8] V. Salas, E. Olias, A. Barrado, and A. Lazaro, "Review of the maximum power point tracking algorithms for stand-alone photovoltaic systems," *Solar energy materials and solar cells*, vol. 90, no. 11, pp. 1555–1578, 2006.
- [9] T. ESRAM, P. L. Chapman *et al.*, "Comparison of photovoltaic array maximum power point tracking techniques," *IEEE Trans. Energy Convers.*, vol. 22, no. 2, p. 439, 2007.
- [10] A. Anurag, S. Bal, S. Sourav, and M. Nanda, "A review of maximum power-point tracking techniques for photovoltaic systems," *International Journal of Sustainable Energy*, pp. 1–24, 2014.
- [11] S. Bal and B. C. Babu, "Comparative study between p&o and current compensation method for mppt of pv energy system," in *Proc. Students Conference on Engineering and Systems*, 2012, pp. 1–6.
- [12] Ankit Gupta, Yogesh K. Chauhan, Rupendra Kumar Pachauri, "A comparative investigation of maximum power point tracking methods for solar PV systems," *Solar Energy*, 136, 2016, pp. 236–253.
- [13] Ganesh Baliram Ingale, Subhransu Padhee, and Umesh Chandra Pati, "Design of stand-alone PV system for DC micro grid" in *Proc. 2016 Int. Conf. Energy Efficient Technologies for Sustainability*, Apr. 2016, pp. 775–780.